In-Ga precursor islands for $Cu(In,Ga)Se_2$ micro-concentrator solar cells

Katharina Eylers[1], Franziska Ringleb[1], Berit Heidmann[2,3], Sergiu Levcenco[2], Thomas Unold[2], Hagen W. Klemm[4], Gina Peschel[4], Alexander Fuhrich[4], Thomas Teubner[1], Thomas Schmidt[4], Martina Schmid[5], Torsten Boeck[1]

1) Leibniz Institute for Crystal Growth, Max-Born-Str. 2, 12489 Berlin, Germany

2) Helmholtz-Zentrum Berlin, Hahn-Meitner-Platz 1, 14109 Berlin, Germany

3) Department of Physics, Freie Universität Berlin, Arnimallee 14, 14195 Berlin, Germany

4) Fritz-Haber-Institut der Max-Planck-Gesellschaft, Faradayweg 4-6, 14195 Berlin, Germany

5) University of Duisburg-Essen and CENIDE, Lotharstr. 1, 47057 Duisburg, Germany

***Abstract* — We present a bottom-up approach for the fabrication of $CuIn_xGa_{(1-x)}Se_2$ (CIGSe) micro-concentrator solar cells by local growth of In-Ga micro-islands. In addition to the intended islands, the indium deposition leads to a parasitic indium wetting layer, which was detected by photoelectron emission microscopy (XPEEM). This layer can be removed by a very short and gentle Ar^+ plasma etching step after indium deposition. The metallic precursor islands were further processed to micro-absorbers and characterized by spatially-resolved photoluminescence measurements for different selenization temperatures. The structural and optoelectronic properties of these absorbers are comparable to those commonly reported for CIGSe films.**

***Index Terms* — $Cu(In,Ga)Se_2$, In-Ga precursor islands, micro-concentrator solar cells, PL measurements, wetting layer, XPEEM.**

I. Introduction

CIGSe is a highly efficient absorber material used for thin-film solar cells. The latest world record efficiency of 22.6 % was reached by the ZSW with a test cell that has an area of 0.5 cm^2 [1]. Due to the rareness of the constituent parts indium and gallium, endeavors to develop a material-saving production process are being made. Micro-concentrator solar cells have the advantage that they require less absorber material, while the cell conversion efficiency can be increased in comparison to full planar absorbers. Compared to macroscopic concentrator solar cells, those micro-concentrators show a better heat dissipation, which reduces thermally caused efficiency losses and allows a more compact module design. The efficiency enhancement of micro-concentrator cells has already been demonstrated for silicon [2] and likewise for CIGSe [3]-[6]. However these achievements were based on top-down approaches for micro-absorber fabrication and thus do not save raw material. For CIGSe these proof-of-principle studies yielded an absolute efficiency increase of up to 4 % [6]. In addition, the first mini-module made of chalcopyrite micro-absorbers showed an absolute efficiency increment of 1.8 % [7].

For material saving, however, a bottom-up process is needed. One such approach, growing the absorber by electrodeposition followed by selenization, has been demonstrated by Sadewasser et al. for circular shaped $CuInSe_2$ absorbers, achieving an efficiency of around 0.3 % [8], and by Duchatelet et al. for linear $Cu(In,Ga)Se_2$ absorbers showing efficiencies up to 7.6 % [9]. Our work focuses on a bottom-up approach based on physical vapor deposition (PVD) on laser patterned substrates. We have previously shown that indium islands can be used as precursors and we have developed a procedure to convert these indium precursors to $CuInSe_2$ micro-absorbers [10]. The local arrangement of the islands, which is indispensable for the alignment of the absorber with the concentrator component, is realized by surface structuring using a femtosecond laser [11]. By adjusting the indium deposition rate and the substrate temperature we are able to control the island size, areal density and aspect ratio to achieve the desired array dimensions [12]. The arrangement of the islands does not play a role for the investigation presented here and therefore we deploy non-laser treated samples with statistically distributed islands.

Here we present results on the integration of gallium into our bottom-up approach for the preparation of CIGSe micro-concentrator solar cells. X-ray photoelectron emission microscopy (XPEEM) measurements to reveal the distribution of In after deposition and after plasma treatment are shown. Furthermore the effect of different selenization temperatures is characterized by photoluminescence (PL) measurements. These PL results are used to determine the Ga content of our absorber-islands.

978-1-5090-5605-7/17/$31.00 ©2017 IEEE

II. Experimental Details

A. Sample preparation

Commercial 50 × 50 × 2 mm^3 soda-lime float glass samples (*Weidner Glas*) served as substrates. Sequential metal deposition was carried out by PVD in a high vacuum chamber enabling both the rear and front heating of the substrate (for details, refer to [11]). Deposition of both, molybdenum and indium was carried out at a substrate temperature of 515 °C. Molybdenum films of 320 nm to 420 nm thickness were deposited at rates between 1 Å/s and 1.8 Å/s. The layer thickness of indium, which was in the range of 90 nm to 110 nm with a deposition rate of 0.3 Å/s, has merely a nominal meaning due to the formation of islands during deposition. Gallium was deposited at a substrate temperature of 370 °C, with a nominal layer thickness of 25 nm to 35 nm and a deposition rate of 0.15 Å/s, which also resulted in the formation of islands. The subsequent copper deposition was carried out at ambient temperature with a rate of 3 Å/s to 5 Å/s, resulting in a homogeneous copper layer of 500 nm thickness. The selenization was performed under UHV conditions using a valve-controlled selenium source that is equipped with a thermal cracking zone operated at 900 °C. The substrate is exposed to Se at room temperature for 30 min. Thereafter, the substrate temperature is increased first to 250 °C and in a second step to values ranging from 500 °C to 560 °C while Se is still evaporated. After cooling down the samples were exposed to an aqueous KCN solution of 0.1 g/mL for 3 min to remove selectively any Cu_xSe_y phases which formed as by-product.

B. Characterization

The PEEM/LEEM measurements were carried out in the SMART microscope operating at the UE49-PGM beamline of the synchrotron light source BESSY II of the Helmholtz Center Berlin (HZB). This aberration corrected and energy filtered instrument combines microscopy (LEEM, PEEM), diffraction (LEED), and spectroscopy (XPS, NEXAFS) techniques for comprehensive characterization of surfaces [13]-[15].

Optical microscopy was performed in bright-field mode with a *Reichert Polyvar 2* microscope equipped with a CCD camera (*Nikon* DS–5 M), a *DS-U1* interface and *NIS-Elements F* imaging software (vers. 3.22). Scanning electron microscopic (SEM) investigations were operated with a *Nova 600 Nanolab DualBeam* microscope from *FEI*, equipped with a TEAM trident analysis system from EDAX. The energy dispersive X-ray diffraction (EDX) measurements were performed in the same SEM system.

For the room temperature photoluminescence (PL) measurements a pulsed laser diode (wavelength: 660 nm, pulse repetition rate: 2.5 MHz) was used as optical excitation source. The PL signals were detected by a 0.5 m Czerny-Turner grating monochromator (grating density: 150 mm^{-1}, spectral resolution: ~0.52 nm) equipped with a liquid N_2 cooled linear InGaAs photodiode array. Spatially and spectrally resolved PL maps were recorded with an exposure time of 2 s, a 1.5 µm step size and an optical excitation spot diameter of ~1.5 µm.

III. Results

A. Indium Wetting Layer

The growth of indium islands on molybdenum coated glass is attended by the formation of a thin indium wetting layer. The existence of a wetting layer was verified by soft XPEEM measurements. Fig.1 shows XPEEM images, representing the spatial distribution of In 3d and Mo 3d photoemission. Figs. 1a and 1b display the same detail on the sample, the edge of an indium island. This is also the case for Figs. 1c and 1d, but an arbitrary area in between the In islands is shown. High intensity regions in the images exhibit a high content of the respective element and vice versa. The exciting X-ray beam has a diameter of 16 × 20 μm^2. On the depicted image section of Figs.1a and 1b the edge of an island can be seen in the upper half of the field of view. The photoelectrons of Mo 3d are not detected in the domain of the island, but at the substrate (Fig. 1a).

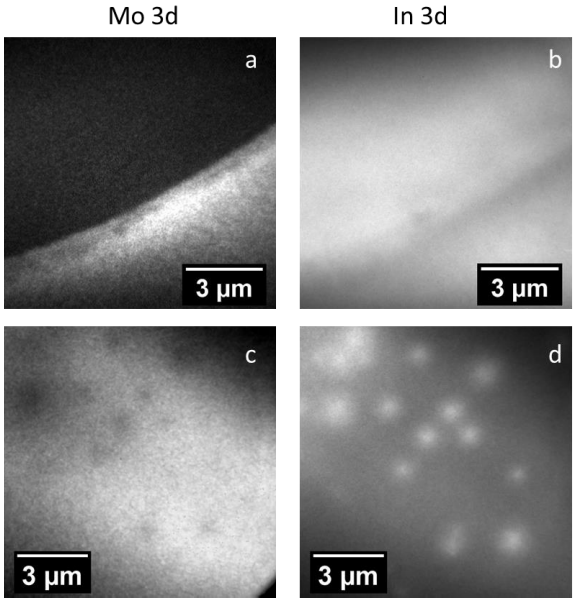

Fig. 1. XPEEM images representing the spatial distribution of Mo 3d (hν = 550 eV) and In 3d (hν = 330 eV) photoemission at a), b) the edge of an indium island (Mo: E_{kin} = 101 eV, In: E_{kin} = 107 eV) and c), d) an arbitrary position on the substrate in between the islands after sputtering (Mo: E_{kin} = 97.5 eV, In: E_{kin} = 108 eV).

In contrast, In 3d photoelectrons are observed within the whole field of view (Fig. 1b). Due to the small mean free path length of the probed photoelectrons at a kinetic energy of

about 100 eV, indium is merely detected within the uppermost 10 Å of the substrate. This implies that the surface is covered with an indium wetting layer of a few angstroms in thickness. This wetting layer is not only detected in the adjacencies of the indium islands, but all over the substrate.

Sequential deposition of In and Ga leads in our case to the formation of interstitial In-Ga structures between the indium islands. We assume that this is related to the interaction of Ga with the In wetting layer. Therefore we analyzed the removal of the wetting layer through sputtering by XPEEM measurements. Figs. 1c and 1d demonstrate the effect of Argon sputtering (U_{Acc} = 450 V, I_S ~ 1 mA, 120 min, with the Argon ions impinging parallel to the surface normal and an exposed sample area of 7 mm in diameter). The photoelectrons of In 3d are no longer detected within the whole field of view, only a few indium spots are still visible. For comparison, the photoelectrons of Mo 3d are observed within the whole field of view. This demonstrates that the indium wetting layer can be removed.

B. Sequential growth of indium-gallium islands

Due to the higher melting and boiling point of indium compared to gallium, a sequential process starting with In and continuing with Ga was used for the preparation of In-Ga micro-islands. For experimental details, please refer to section II. On the resulting samples gallium was mainly detected at the edge of indium islands, in a fringe around an indium rich core. This phenomenon is illustrated by the energy dispersive X-ray (EDX) maps shown in Fig. 2.

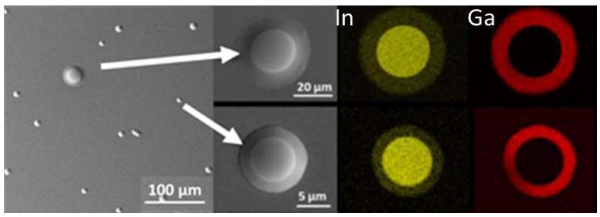

Fig. 2. SEM images (left) and EDX maps (right) of In-Ga micro islands.

The observed phase segregation within the In-Ga islands is in line with the solidification behavior of the eutectic In-Ga system and thus indicates that the solidification process is rather thermodynamically than kinetically dominated. In addition, small interstitial islands of about 5 µm in diameter have formed, which also consist of an indium-rich core surrounded by a gallium-rich fringe. We presume, that these smaller islands form during gallium deposition due to the interaction of Ga atoms approaching the surface from the vapor phase with the indium wetting layer.

For the fabrication of well-defined arrays of CIGSe micro-absorbers the formation of interstitial islands has to be avoided. Since the XPEEM measurements showed the potential to remove the indium wetting layer, we introduced an additional Ar^+ plasma etching step to remove the wetting layer prior to the deposition of Ga. As the wetting layer is only a few angstroms thick, a very gentle, short etching is sufficient to suppress the formation of any interstitial structures (Fig. 3).

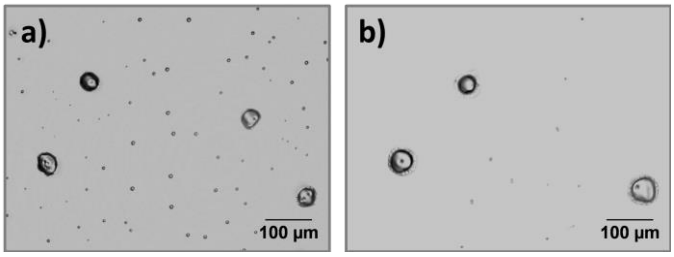

Fig. 3. Light micrographs of a) Sample with In-Ga islands without additional Ar^+ plasma etching step prior to Ga deposition b) Sample with additional Ar^+ plasma etching step to remove the indium wetting layer.

We assume that a higher diffusivity of Ga atoms on the bare Mo than on an In wetting layer causes this desirable outcome. In the following we show that this horizontally inhomogeneous In-Ga distribution throughout the metallic precursor can be eliminated in the subsequent selenization step.

C. Processing to Cu(In,Ga)Se₂ micro-islands

Gallium is not only taken up by the indium islands, but also forms a wetting layer itself. Fig. 4a shows the edge of an In-Ga island and the Ga wetting layer, which has a ripple structure and appears to be ticker than the In wetting layer. Thus, for the further processing to chalcopyrite absorber islands, the samples with the In-Ga precursors were again treated with a gentle Ar^+ plasma etching step. The samples were then coated with copper and selenized, as described in the experimental section. In Fig. 4b an example of one single resulting micro-absorber island obtained after selective etching of copper selenides is depicted.

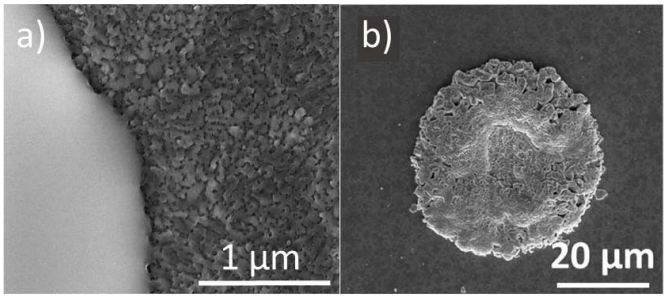

Fig. 4. SEM images of a) In-Ga island edge with Ga wetting layer and b) one single $Cu(In,Ga)Se_2$ micro-island selenized under UHV conditions and etched in a KCN solution.

D. Photoluminescence measurements

Photoluminescence measurements were carried out on samples, which were prepared applying different selenization temperatures. The optical band gap energy of $CuInSe_2$ is ~1.04 eV. By replacing In atoms with Ga atoms the band gap can be increased to up to ~1.68 eV, which is the optical band gap energy of $CuGaSe_2$ [16]. In Figs. 5a-d maps of the PL peak position are shown for CIGSe islands prepared under identical conditions, except for the maximum selenization temperature (500 °C (I), 520 °C (II), 540 °C (III) and 560 °C (IV)). It has to be considered that with the wavelength of the optical excitation source (660 nm) and the absorption coefficient of CIGSe ($\alpha = 8 \times 10^{-4}$ cm^{-1} at 1.9 eV [21]) the penetration depth of the PL measurements yields approximately 100 nm, i.e. only the surface region of the absorber is probed.

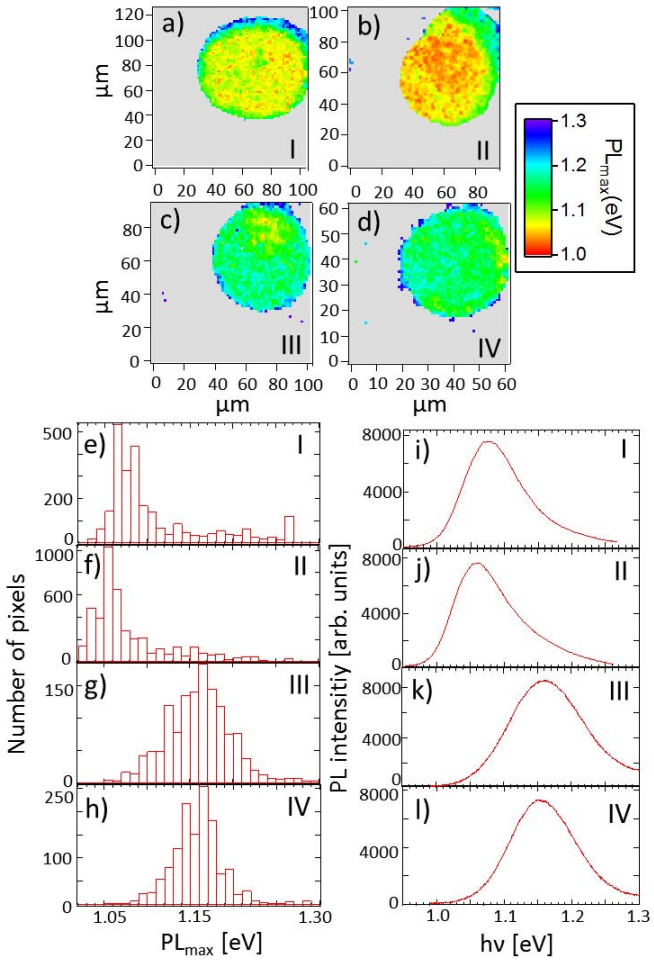

Fig. 5. a)-d) PL maps of the peak emission energies, for CIGSe islands selenized at 500 °C (I), 520 °C (II), 540 °C (III) and 560 °C (IV). e)-h) Statistical analysis of the PL maps for samples I-IV. i)-l) Averaged spectra of I-IV as a function of energy.

The detection range was chosen such that photoemission spectra could be measured across the entire island area. The peak energy is depicted by a color code ranging from red for the lower limit (1.0 eV) to purple for 1.3 eV. Samples produced with lower substrate temperatures during selenization (I-II) show a wide range of emission maxima (1.04 eV - 1.15 eV) in photoluminescence maps. High energy emission indicating a high Ga content is detected at the edges of the islands, whereas low energy emission, indicative of an indium rich phase, is observed in the center. This emission distribution reflects the horizontal elemental distribution of indium and gallium in the segregated In-Ga precursor islands and indicates a poor migration of both metals within the islands during the selenization process. In contrast, samples which were exposed to higher substrate temperatures during selenization (III-IV) show promising results regarding In-Ga intermixing, which is an important prerequisite for optimizing the absorber.

A statistical analysis of each PL map depicted in Figs. 5a-d is shown as histogram in Figs. 5e-h. Figs. 5i-l show the averaged spectra, from all PL spectra in the region of the corresponding CIGSe islands of Figs. 5a-d. The position of the main peak of the averaged spectra (Figs. 5i-l) shifts from approximately 1.05 eV to 1.16 eV with increasing temperature. The band gap for samples with higher substrate temperatures during selenization is comparable with ideal values for common thin-film CIGSe absorbers reported in the literature [17] and is clearly shifted upwards in comparison with the band gap of previously measured CISe micro-islands (1.03 eV, data not shown). Several studies have shown the correlation between Ga content and band gap in CIGSe [18]-[21]. We used equation (1) from [21] to estimate the Ga content in the investigated absorber volume of our CIGSe islands.

$$E_g(x) = 1.010 + 0.626x - 0.167x(1-x) \qquad (1)$$

The authors of [21] obtained this approximation by fitting a function based on theoretical models on experimental data obtained from samples of varying In-Ga content. By inserting the PL peak position into Eq. 1 we calculated the approximate Ga content of the CIGSe islands. In Fig. 6 the results of this calculation are illustrated for all samples. Samples with a lower substrate temperature during Se evaporation (I and II) have a lower average Ga content in the probed absorber volume of about 0.08 to 0.14, compared to samples III and IV which were selenized at higher temperatures, exhibiting a Ga content of about 0.28 to 0.30. Since the best solar cells contain ~30 % Ga [1], [22]-[23], we aim for a composition of $CuIn_{0.7}Ga_{0.3}Se_2$. For our CIGSe micro-absorber islands this ratio can be achieved by higher substrate temperatures (III-IV) during Se evaporation.

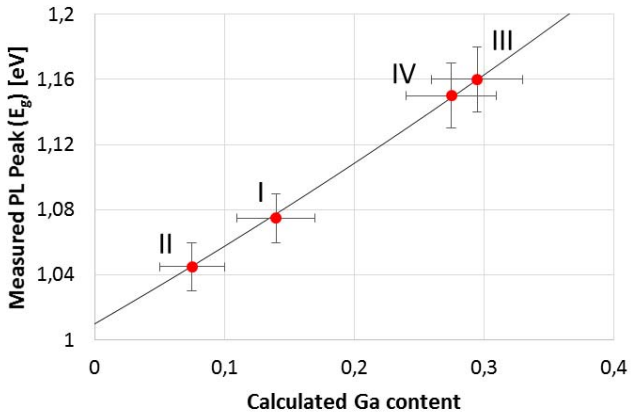

Fig. 6. Diagram of the calculated Ga content of the $Cu(In,Ga)Se_2$ micro-absorbers as a function of the average measured PL peaks of samples I-IV. The error bars indicate the measured range of PL peaks and the therefore resulting range of Ga content. The line indicates Eq. (1).

III. Discussion

Sequentially grown In-Ga precursor islands can be transformed into $CuIn_xGa_{(1-x)}Se_2$ micro-absorbers, which in turn will be further processed to CIGSe micro-concentrator solar cells. The removal of the indium wetting layer, which arises during indium island growth, clearly improves the sample quality by suppressing additional interstitial island growth during the subsequent deposition of gallium. Samples produced with high selenization temperatures (540 °C – 560 °C) show promising results regarding homogeneity and band gap of the resulting CIGSe micro absorbers due to a better mixing of the components. We have so far obtained valuable information about the horizontal surface homogeneity of the islands by PL mapping, but it is well known from the literature [24-26] that absorber may have a Ga gradient and it has yet to be verified experimentally in our micro-absorbers.

IV. Summary

We demonstrated a bottom-up approach for the local growth of In-Ga islands, which can be used as precursors for the fabrication of chalcopyrite micro-absorbers. We verified the existence of an indium wetting layer and introduced an approach to remove it. Photoluminescence measurements were performed on samples, which were prepared applying different selenization temperatures and the results were used to determine the Ga content of our absorber-islands.

Our approach combines the potential for material saving by a bottom-up process with the advantage of vacuum evaporation, which currently yields the highest efficiencies for CIGSe solar cells.

Acknowledgement

The authors thank HZB for the allocation of synchrotron radiation beamtime. Furthermore we gratefully acknowledge financial support by the Deutsche Forschungsgemeinschaft (DFG, German Research Foundation) through BO1129/6-1 and SCHM2554/3-1. The research leading to these results has received funding from the European Union Seventh Framework Program (FP7/2007-2013) under grant agreement no. 609788.

References

[1] P. Jackson, R. Wuerz, D. Hariskos, E. Lotter, W. Witte, M. Powalla, *Phys. Status Solidi RRL,* 2016, 10, No. 8, 583–586
[2] J. Yoon, A. J. Baca, S. I. Park, P. Elvikis, J. B. Geddes, 3rd, L. Li, R. H. Kim, J. Xiao, S. Wang, T. H. Kim, M. J. Motala, B. Y. Ahn, E. B. Duoss, J. A. Lewis, R. G. Nuzzo, P. M. Ferreira, Y. Huang, A. Rockett, J. A. Rogers, *Nature Materials*, 2008, 7,907.
[3] M. Paire, L. Lombez, F. d. r. Donsanti, M. Jubault, S. p. Collin, J.-L. Pelouard, J.-F. o. Guillemoles, D. Lincot, *Journal of Renewable and Sustainable Energy,* 2013, 5, 011202.
[4] B. Reinhold, M. Schmid, D. Greiner, M. Schüle, D. Kieven, A. Ennaoui, M. C. Lux-Steiner, *Progress in Photovoltaics: Research and Applications*, 2015, 23, 1929.
[5] M. Paire, A. Shams, L. Lombez, N. Péré-Laperne, S. Collin, J.-L. Pelouard, J.-F. Guillemoles, D. Lincot, *Energy & Environmental Science*, 2011, 4, 4972.
[6] M. Paire, L. Lombez, N. Pere-Laperne, S. Collin, J.-L. Pelouard, D. Lincot, J.-F. Guillemoles, *Applied Physics Letters* 98, 264102, 2011.
[7] S. Jutteau, J.-F. Guillemoles, M. Paire, *Applied Optics*, Edition edn., 2016.
[8] S. Sadewasser, P. M. P. Salome, H. Rodriguez-Alvarez, *Sol. Energy Mat. Sol. Cells,* 159, 496, 2017.
[9] A. Duchatelet, K. Nguyen, P.-P. Grand, D. Lincot, and M. Paire, *Applied physics letters*, 109, 253901, 2016.
[10] T. Boeck, F. Ringleb, R. Bansen, *Crystal Research and Technology,* 1600239, 2017.
[11] F. Ringleb, K. Eylers, T. Teubner, T. Boeck, C. Symietz, J. Bonse, S. Andree, J. Krüger, B. Heidmann, M. Schmid, M. Lux-Steiner, *Applied Physics Letters*, 108, 111904, 2016.
[12] F. Ringleb, K. Eylers, Th. Teubner, H.-P. Schramm, C. Symietz, J. Bonse, S. Andree, B. Heidmann, M. Schmid, J. Krüger, T. Boeck, *Applied Surface Science*, 2016. http://dx.doi.org/10.1016/j.apsusc.2016.11.135
[13] R. Wichtendahl, R. Fink, H. Kuhlenbeck, D. Preikszas, H. Rose, R. Spehr, P. Hartel, W. Engel, R. Schlögl, H.-J. Freund, A.M. Bradshaw, G. Lilienkamp, T. Schmidt, E. Bauer, G. Benner, E. Umbach, *Surface Review and Letters 05*, 1249, 1998.
[14] Th. Schmidt, H. Marchetto, P.L. Lévesque, U. Roh, F. Maier, D. Preikszas, P. Hartel, R. Spehr, G. Lilienkamp, R. Fink, E. Bauer, H. Rose, E. Umbach, H.-J. Freund, *Ultramicroscopy 110*, 1358 – 1361, 2010
[15] Th. Schmidt, A. Sala, H. Marchetto, E. Umbach, H.J. Freund, *Ultramicroscopy 126*, 23, 2013.
[16] L. Shay, J. Wernick, *Ternary Chalcopyrite Semiconductors*, Pergamon, Oxford, 1975.
[17] S. Shirakata, T. Nakada, *Thin Solid Films 515*, 6151 - 6154, 2007.
[18] S.-H. Wei, A. Zunger, *Journal of Applied Physics 78* (6) 3846 - 3856, 1995.

[19] S.-H. Wei, S. B. Zhang, A. Zunger, *Physics Letters 72* (24) 3199-3201, 1998.
[20] M. Turcu, I. M. Kötschau, U. Rau, *Journal of Applied Physics 91* (3), 1391-1399, 2002.
[21] M. I. Alonso, M. Garriga, C. A. Durante Rincón, E. Hernández, and M. León, *Applied Physics A: Materials Science & Processing A74*, 659, 2002.
[22] J. Hedstrom, H. J. Olsen, M. Bodegard, A. Kylner, L. Stolt, D. Hariskos, M. Ruckh, and H. W. Schock, *Proceedings of the 23rd IEEE Photovoltaic Specialists Conference*, p. 364, 1993.
[23] A. M. Gabor, J. R. Tuttle, D. S. Albin, M. A. Contreras, R. Noufi, and A. M. Hermann, *Applied physics letters 65*, 198, 1994.
[24] M. Marudachalam, R. W. Birkmire, H. Hichri, J. M. Schultz, A. Swartzlander, M. M. Al-Jassim, *Journal of Applied Physics 82*, 2896, 1997.
[25] R. Mainz, A. Weber, H. Rodriguez-Alvarez, S. Levcenko, M. Klaus, P. Pistor, R. Klenk, H.-W. Schock, *Progress in Photovoltaics: Research and Applications* 23:1131–1143, 2014.
[26] W. Witte et al., *Progress in Photovoltaics: Research and Applications,* 23:717–733, 2015